

# On the effect of intramolecular H-bonding in the configurational assessment of polyhydroxylated compounds with computational methods.

## The hyacinthacines case.

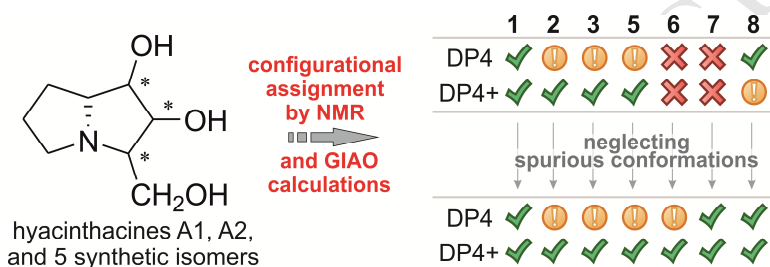
María Marta Zanardi<sup>1,2</sup>, Maximiliano A. Sortino,<sup>2</sup> and Ariel M. Sarotti<sup>3\*</sup>

<sup>1</sup> Facultad de Química e Ingeniería del Rosario, Pontificia Universidad Católica Argentina, Av. Pellegrini 3314, Rosario 2000, Argentina.

<sup>2</sup> Área Farmacognosia, Facultad de Ciencias Bioquímicas y Farmacéuticas, Universidad Nacional de Rosario, Suipacha 531, Rosario 2000, Argentina

<sup>3</sup> Instituto de Química de Rosario, Facultad de Ciencias Bioquímicas y Farmacéuticas, Universidad Nacional de Rosario - CONICET, Suipacha 531, S2002LRK Rosario, Argentina. [sarotti@iquir-conicet.gov.ar](mailto:sarotti@iquir-conicet.gov.ar)

### ABSTRACT



Hyacinthacines are important members of the pyrrolizidine family, with several compounds having ambiguous, revised or unverified structures. Herein we thoroughly explored the performance DP4 and DP4+ for the *in silico* stereoassignment of hyacinthacines A2, A2 and five synthetic isomers. The results suggested that the quality of the predictions strongly depended on the conformational landscape provided by DFT energies, with five compounds correctly assigned. In the two cases incorrectly classified we found that the source of the problem was conformational in nature, with spurious conformations being considerably over-stabilized by intramolecular H-bondings. We showed that neglecting such shapes resulted in a noteworthy improvement, with all compounds correctly assigned in high confidence (>99.9%).

**Keywords:** DP4+, hyacinthacines, pyrrolizidines, H-bonding

### 1. Introduction

In the last decades, iminosugars (also termed azasugars) have received much interest mainly because their promising biological activities [1]. Particularly, polyhydroxylated alkaloids that mimic the structures of sugars are widespread in plants and have been shown to inhibit glycosidases. These enzymes are involved in several important anabolic and catabolic processes, playing an essential role in a wide variety of diseases.

The inhibition is due to the structural resemblance of their sugar moiety to natural substrates. Thus, glycosidase-inhibiting iminosugars could have enormous potential applications as biochemical tools and therapeutic agents [2].

Naturally occurring iminosugars are classified into five structural classes: polyhydroxylated pyrrolidines, piperidines, indolizidines, pyrrolizidines, and nortropans [1]. An important group of polyhydroxylated pyrrolizidine alkaloids are the hyacinthacines, characterized by a common 7a-*R*-hydro-1,2-dihydroxy-3-hydroxymethylpyrrolizidine core (Figure 1) [3]. The different hyacinthacine alkaloids can be classified according to the substituents present at C-5 (H, Me or  $-\text{CH}_2\text{OH}$ ), C-6 (H or OH) and C-7 (H or OH) in ring B. To date, 19 different members of the family were isolated from extracts of the *Hyacinthaceae* family, and were named A<sub>1-7</sub>, B<sub>1-7</sub> and C<sub>1-5</sub> (where A, B and C accounts for the number of 0, 1 or 2 hydroxyl /hydroxymethyl groups present at ring B, respectively) [2-5].

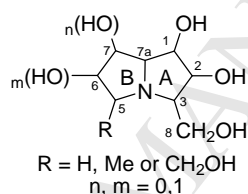


**Figure 1.** General structure of the hyacinthacine alkaloids.

The structures of natural hyacinthacines have been determined mainly from NMR analysis. Hence, given the complexity and variety of these compounds, it is not surprising to find cases of structural ambiguities, which seems to be often the case in the field of natural products [6]. For example, in 2007 Kato *et al.* reported the isolation of hyacinthacine C4 (Figure 2) [7], with identical structure to the previously isolated hyacinthacine C1 [8], but with clearly different NMR data.

Because of the lack of X-ray crystallographic structures of the natural isolates, coupled with the structural complexity, total synthesis has emerged as the only alternative of stereochemical validation [5]. Some of the natural hyacinthacines were proved by synthesis, like A1-A3, A6, A7, B1-B5 and C2 [1,5], whereas compounds A4, A5, B6, C1 and C4 have not been synthesized yet. On the other hand, the putative structures of some members were rejected by total synthesis due to inconsistencies between the spectroscopic data of natural and synthetic material, as in the case of B7, C3 and C5 (Figure 2) [9,10].

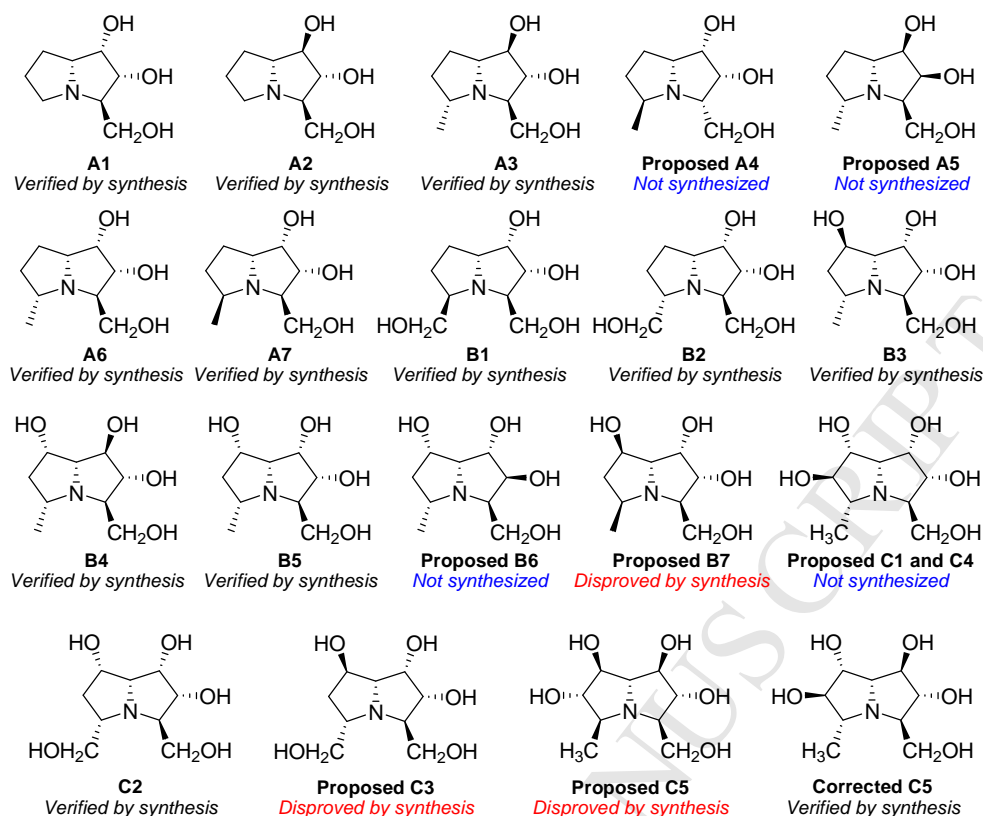


Figure 2. Naturally occurring hyacinthacines

Naturally occurring hyacinthacines are not the only examples of structural ambiguity or revision. Several unnatural isomers have also been prepared either as part of the structural assignment or for medicinal chemistry purposes [3], and in some cases the putative synthetic structures had to be further corrected. For example, during the synthesis of unnatural isomers of A1 and A2 the structures of some compounds were initially reported wrongly [11a], later revised by the same group some years later [11b] (*vide infra*).

In the last years, the number of publications demonstrating the convenience on the use of quantum computational calculations of NMR shifts to solve structural and stereochemical issues has significantly increased [12]. Among the different methodologies available to facilitate the assignment (including CP3 [13], DP4 [14], ANN-PRA [15], Case 3D [16], DU8+ [17], and DiCE [18]), we have introduced the DP4+ probability as a suitable toolbox to determine the most likely structure of a target molecule when only one set of experimental NMR data is available [19]. DP4+ is an updated version of the popular DP4 method developed by Goodman [14], and includes the probability descriptors of both scaled and unscaled shifts. The other major

difference between both methods is related with the level of theory employed to compute the NMR shifts. In particular, whereas in DP4 the GIAO calculations are done using MMFF optimized geometries (highly convenient in terms of computational cost) [14], DP4+ requires an additional geometry optimization at B3LYP/6-31G\* level [19]. Despite the greater CPU time involved, we showed that both modifications are needed to improve the performance of the method [19-20]. Nevertheless, both methods should be taken as complements, as the fast DP4 calculations can be used to guide the *in silico* assignment, further refined by DP4+ [21].

Irrespective the mathematical strategy behind the data correlation, it must be emphasized that in all cases the certainty of the assignment is strongly related with the quality of the NMR prediction itself. Structures featuring poorly computed NMR shifts are expected to be classified as unlikely, regardless whether they are correct or not [14,19]. On this subject, the molecular flexibility imposes an additional problem, as the calculated NMR values are the result of the conformational averaging, typically carried out using Boltzmann analysis [12]. Hence, whenever the computed conformational landscape significantly differs from the experimental one, a potential drawback could be foreseen. In the case of common non-polar organic compounds with relatively low conformational freedom the contribution exerted by each rotamer can be well estimated from the energies calculated at DFT levels, affording typically accurate NMR simulations and further safe assignment [12b]. The scenario is, however, quite different when dealing with highly polar molecules bearing multiple H-bonding groups whose NMR spectra are recorded in polar solvents such as D<sub>2</sub>O, MeOH-d<sub>4</sub> or DMSO-d<sub>6</sub>. In these cases, it is well known that DFT energies tend to favor conformers with intramolecular H-bonding, which in turn could offer a distorted description of the system [12b].

The real conformational behavior of polyalcohols is strongly governed by H-bonding interactions, which could take place both intra- and intermolecularly, giving rise to complex temporal dynamics [22]. In addition, the medium properties can influence the H-bonding, affecting both the energy and geometry of the system, and representing the main difficulty associated with the quantum-based NMR calculations of such type of molecules [23]. It was pointed that the effect of the solvent on the NMR shifts of the solute is indirect, with the solvent affecting the conformational distribution of the solute, in turn modifying the isotropic shielding values [24]. The use of molecular dynamics

has also been explored to explicitly account for the solvent effect [24-25], though these methods are too computationally demanding for structural elucidation purposes. The explicit inclusion of few solvent molecules for further DFT treatment would also result in a considerable increase in the overall computational cost given the number of solute/solvent configurations to take into account. On the other hand, the effect of the solvent can be included implicitly, typically using the PCM or related solvation models [25]. A substantial amount of computational work has demonstrated that the NMR shifts of a wide variety of carbohydrates can be well estimated from DFT or *ab initio* calculations [25]. For that reason, it is by far the most common approach to include solvent effect in the field of DFT calculations of NMR shifts.

In an effort to understand the scope and limitations of DP4 and DP4+ in the stereoassignment of iminosugars, we turned our attention to the hyacinthacine family, with many congeners incorrectly assigned in the recent past and many others suggested though not confirmed. In this work, we wish to illustrate the achievements and difficulties surrounding our journey to pursue our goals.

## Results and Discussion

We started our study by evaluating DP4 and DP4+ to establish the relative configuration of the simplest members of the hyacinthacine family, containing substituents only at ring A and leading to 8 possible diastereoisomers (Figure 3). After an exhaustive literature search, we could find the experimental NMR data of seven compounds, including **1** (A1), **2** (A2), and five other synthetic isomers (**3**, **5**, **6**, **7** and **8**) [11,26]. As discussed above, the compounds **3** and **6** were initially reported as **5** and **4** [11a], respectively, later revised in 2010 [11b]. However, since the NMR shifts of the revised **3** and **6** were not reported again after the final revision, we took the experimental values from the original reference.

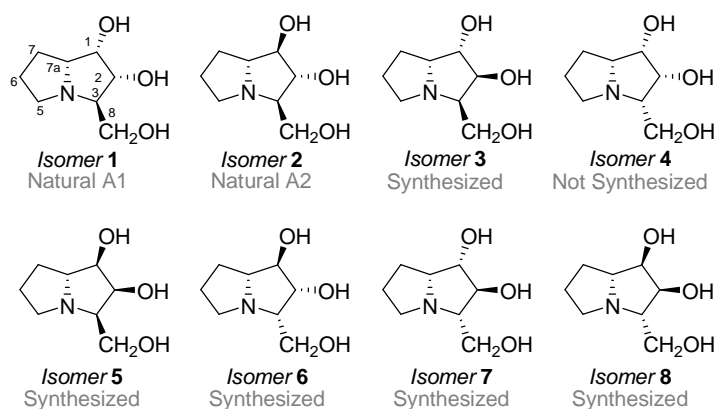


**Figure 3.** Structures of the eight possible diastereoisomers of natural hyacinthacines A1 (**1**) and A2 (**2**). Apart from the two naturally occurring A1 and A2, the NMR data of synthetic **3**, **5**, **6**, **7** and **8** were also available.

Initially, an exhaustive conformational sampling of compounds **1-8** was carried out with the MMFF<sub>aq</sub> force field implemented in Macromodel [27]. To prevent missing potentially relevant conformations, all conformers found within 10 kcal/mol from the global minima were kept for further NMR and/or geometry optimization calculations. The number of unique conformations located oscillated around 150 per isomer. All conformers were next submitted to a geometry optimization at the PCM/B3LYP/6-31G\* using water as solvent, and after removing duplicates, all optimized structures were submitted to the NMR calculation stage. The NMR calculations were carried out at the B3LYP/6-31G\*\*//MMFF level (for DP4 analysis) and PCM/mPW1PW91/6-31+G\*\*//B3LYP/6-31G\* level (for DP4+ analysis). The isotropic shielding values were finally Boltzmann averaged using the SCF relative energies obtained from the NMR calculations.

When correlating the calculated NMR values of **1-8** with the experimental data available for seven isomers under study (**1-3**, **5-8**) using DP4 we noticed that only four compounds were correctly assigned (**1**, **2**, **3** and **8**), two of them in high confidence (**1** and **8**). The remaining 3 examples (**5**, **6** and **7**) were incorrectly assigned, being compound **2** systematically pointed as the most likely structure. Noticeably, the DP4 probabilities computed for **6** and **7** when using the experimental NMR data of them were surprisingly low (<0.1%), with the correct structures being ranked at 7<sup>th</sup> and 6<sup>th</sup> position, respectively. As expected, the results improved with DP4+, with five compounds correctly assigned (**1**, **2**, **3**, **5** and **8**), most of them in high confidence. Surprisingly, here again compounds **6** and **7** afforded unusually bad results (DP4+ < 0.1%), being the **5** and **4** isomers the most probable ones, respectively. The

corresponding right structures of **6** and **7** were very poorly ranked, taking the 5<sup>th</sup> and 6<sup>th</sup> positions, respectively, which in our experience represented a highly unusual result. In an effort to understand this sharp failure of DP4/DP4+ in the stereoassignment of **6** and **7** we thoroughly revised the experimental NMR data reported for both, but we could not find any evident source of error. Therefore, we concluded that the problem arose during the NMR calculation stage. The corrected mean absolute errors (CMAE, defined as  $\sum_n |\delta_{\text{scaled}} - \delta_{\text{exp}}|/n$ ) and corrected maximum errors (CMaxErr,  $\max |\delta_{\text{scaled}} - \delta_{\text{exp}}|$ ) were much higher for **6** and **7** than those obtained for the remaining isomers. For instance, at the PCM/mPW1PW91/6-31+G\*\*//B3LYP/6-31G\* both **6** and **7** displayed the highest <sup>13</sup>C-CMAE and <sup>13</sup>C-CMaxErr values (2.70 ppm and 5.20 ppm, respectively, for **6**, and 2.80 ppm and 6.70 ppm, respectively, for **7**). On the other hand, the corresponding values calculated for **1-3**, **5** and **8** were considerably lower (<sup>13</sup>C-CMAE range: 1.50-2.00 ppm, <sup>13</sup>C-CMaxErr range: 3.00-4.40 ppm). Similar trends were noticed for the proton shifts, with <sup>1</sup>H-CMAE values of 0.27 and 0.24 ppm for **6** and **7**, respectively, doubling the results obtained for **1-3**, **5** and **8** (0.104 ppm in the average). Such a modest estimation of the NMR shifts of **6** and **7** accounted for the low DP4/DP4+ probabilities calculated after correlating the theoretical NMR data with the experimental shifts of both.

**Table 1.** DP4 and DP4+ probabilities, and CMAE and CMaxErr values computed after correlating the experimental NMR data of compounds **1-3** and **5-8** with the calculated NMR shifts of **1-8**.

Comp.	Probability (rank) <sup>a</sup>	CMAE <sup>b</sup>		CMaxErr <sup>b</sup>	
		<sup>13</sup> C	<sup>1</sup> H	<sup>13</sup> C	<sup>1</sup> H
<b>DP4</b>					
<b>1</b>	>99.9 (1°)	1.10	0.12	2.20	0.35
<b>2</b>	59.7 (1°)	2.10	0.14	3.40	0.34
<b>3</b>	51.3 (1°)	1.40	0.15	3.80	0.43
<b>5</b>	43.6 (2°)	1.20	0.15	2.20	0.26
<b>6</b>	<0.1 (7°)	3.10	0.42	7.20	0.93
<b>7</b>	<0.1 (6°)	2.90	0.24	6.50	0.56
<b>8</b>	98.7 (1°)	1.80	0.14	3.40	0.31
<b>DP4+</b>					
<b>1</b>	>99.9 (1°)	1.5	0.12	3.9	0.41
<b>2</b>	>99.9 (1°)	1.5	0.10	3.5	0.31
<b>3</b>	97.7 (1°)	2.0	0.09	4.4	0.24
<b>5</b>	>99.9 (1°)	1.8	0.07	3.2	0.19
<b>6</b>	<0.1 (5°)	2.7	0.27	5.2	0.58
<b>7</b>	<0.1 (6°)	2.8	0.24	6.7	0.55
<b>8</b>	59.6 (1°)	1.5	0.14	3.0	0.28

a) Indicates the ranked position of the correct isomer according to the probability values.

b) Computed by correlating the NMR data calculated for the corresponding isomer from which the experimental NMR were taken (ie. calcd. **1** vs exp. **1**)

To understand the origins of these findings, we hypothesized that the disagreement should be conformational in nature, with the contribution of spurious conformations

overestimated by DFT calculations. In this regard, the conformational analysis of substituted pyrrolizidine systems has received considerable attention. Early investigations recognized that the pyrrolizidine nucleus could exist in either an *exo*-buckled (**X** type, Figure 4) or *endo*-buckled (**N** type) conformations based on NMR data and crystallographic studies [28]. In addition, due to the plausible nitrogen inversion path the bicyclic system could be *cis* or *trans*-fused depending on the relative orientation of the bridgehead proton (H-7a) with the nitrogen lone pair. The lower angular strain typically makes the *cis* conformations more stable than the *trans*-fused ones, though it was pointed that the *cis/trans* ratio strongly depends on the type and relative orientation of the substituents [29]. According to our DFT calculations, there are four representative types of conformations for the pyrrolizidine core, with Figure 4 showing the B3LYP/6-31G\* optimized structures found after exhaustive exploration of the potential energy surface (PES). The **X** and **N** conformations feature the two five-membered rings *exo* or *endo*, respectively, whereas the **X/N** shape consists on one pyrrolizidine being *exo* and the other one *endo*. Apart from these *cis*-fused structures, we also found the corresponding *trans*-fused structure **T**. The **X** is the most stable conformation of the bicyclic system, being 2.1 Kcal/mol lower in energy than the **N** shape, with the intermediate **X/N** geometry lying in between ( $E_{\text{rel}} = 0.5$  Kcal/mol), whereas the **T** shape is highly unstable ( $E_{\text{rel}} = 3.7$  Kcal/mol). These results were in nice agreement with Belostotskii's findings [30], and were further validated by us at the M06-2X/6-311+G\*\* level.

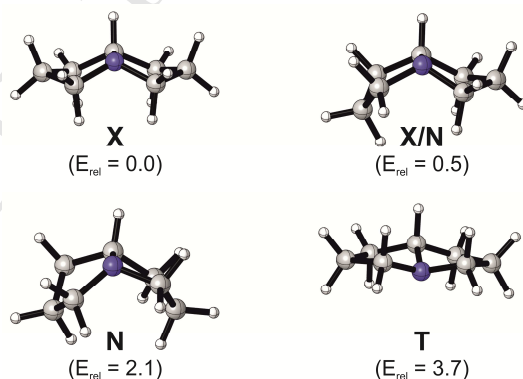


**Figure 4.** B3LYP/6-31G\* optimized conformations of the pyrrolizidine ring. The relative energies are given in Kcal/mol.

With this interesting background in mind, we next explored the global minima conformations found for compounds **1-8** at the PCM/mPW1PW91/6-31+G\*\*//B3LYP/6-31G\* level of theory. The results showed a clear conformational/configurational dependences mainly dictated by the intramolecular H-

bonding arrays (Figure 5). The *cis*-fused conformations were the global minima of compounds **1-3** (**X** type), **7** (**X** type) and **5** (**X/N** type), whereas the *trans*-fused structures were the most stable conformations of compounds **4**, **6** and **8**. The higher stability of **T** shapes is mainly due to a forced H-bond between the OH group at C-8 with the lone pair of the N atom, as previously suggested by Skvortsov [29b]. In fact, with the only exception of isomers **7** and **8**, such H-bonding was present in all the remaining global minima geometries highlighting its relevance in the DFT-based conformational preference of this type of compounds. Moreover, only the isomers with C-3*S* configuration (compounds **4**, **6**, **7** and **8**) showed significantly populated **T** structures because of the adequate geometrical disposition of the N lone pair and C-8-OH group to form non-covalent interactions. In the corresponding C-3*R* epimers the **T** shapes are not stabilized because of the impossibility of H-bonding formation. Curiously, the four isomers correctly assigned by DP4+ in high confidence (**1-3** and **5**) have the C-3*R* configuration (with no energetically available **T** shapes), whereas the isomers misassigned (**6** and **7**) or assigned in low confidence (**8**) by DP4+ are C-3*S* configured with significantly populated **T** forms.

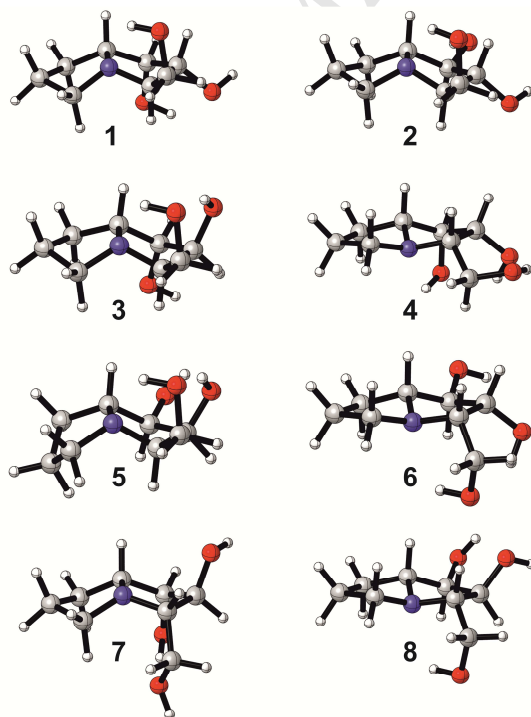


**Figure 5.** Global minima conformations of compounds **1-8** located at the PCM/mPW1PW91/6-31+G\*\*//B3LYP/6-31G\* level of theory.

With the intention of finding a possible dependence on the quality of NMR prediction with the pyrrolizidine shape, we computed the mean absolute errors (MAE, defined as  $\text{abs}[\delta_{\text{exp}} - \delta_{\text{calc}}]$ ) arising from each individual conformations of compound **6** (164 in total),

and arranged the data in terms of conformation type of the pyrrolizidine core. In agreement with our hypothesis, the higher discrepancies were computed for the **T** shapes, mainly in the case of proton data. Interestingly, in the case of **6** the T-shapes account for the 95% of the Boltzmann populations.

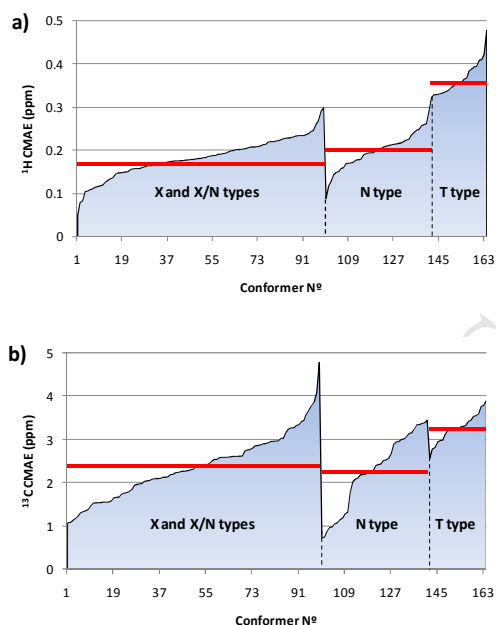


**Figure 6.**  $^1\text{H}$  (above) and  $^{13}\text{C}$  (below) CMAE values obtained by correlating the NMR shifts computed for each individual conformer of **6** at the PCM/mPW1PW91/6-31+G\*\*//B3LYP/6-31G\* level of theory with the experimental NMR shifts reported for **6**. For clarity, the CMAE values were sorted in ascending order of magnitude for each type of conformations (X and X/N, N and T). The horizontal red line indicates the averaged CMAE values for each type of conformation.

In the case of compound **7**, the situation became more complex. Apart from the same problem experienced with **T** shapes (in this case, accounting for the 49% of the Boltzmann population), we also found an additional conflicting conformations arising from intramolecular H-bonding between the OH groups at C-1 and C-8. In these highly contributing conformations (40% of the Boltzmann population) the pyrrolizidine core is **X** shaped, featuring the three substituents at C-1, C-2 and C-3 in *pseudo*-axial positions (hence termed **X<sub>ax</sub>**, see compound **7**, Figure 5). Despite in principle such arrangement would not seem unexpected, it showed poor match with the scalar couplings reported for **7**. In particular, the experimental  $^3J_{2,3}$  is 9.3 Hz, indicating a clear *pseudo*-diaxial disposition of both protons [11b]. However, in the **X<sub>ax</sub>** shapes the dihedral angles between H-2 and H-3 are close to  $90^\circ$ , which should yield an almost null coupling according to the Karplus equation. Since the H-2/H-3 dihedral angles of the **T** conformations are also near  $90^\circ$ , and considering that the **T** and **X<sub>ax</sub>** shapes account for

the 89% of the Boltzmann population, the computed  $^3J_{2,3}$  value was 3.6 Hz, much lower than the experimental one.

According to our analysis the modest reproduction of the NMR shifts was related, at least in part, with the unexpectedly high contributions of **T** and **X<sub>ax</sub>** conformations (particularly important in compounds **4**, **6**, **7** and **8**). In order to understand if such trend could be an artifact of the PCM/mPW1PW91/6-31+G\*\*//B3LYP/6-31G\* level, we decided to explore the conformational landscape of compound **7** at different levels of theory. To avoid the daunting task of reanalyzing the conformational preference of all rotamers, we narrowed the analysis by selecting four representative conformations of **7** (Figure 7). Compound **7-c67** (**X<sub>ax</sub>** shaped) is the global minima found at the DP4+ level (PCM/mPW1PW91/6-31+G\*\*//B3LYP/6-31G\*), **7-c136** (**T** shaped) is the second most stable conformation of **7**, and **7-c4** and **7c-10** are the first two more stable structures of **7** appearing with not **T** nor **X<sub>ax</sub>** shapes. It has been shown that B3LYP might afford modest results when dealing with conformational studies of saccharides [31]. For that reason, apart from increasing the basis set size (6-311+G\*\*) the geometries of these structures were fully reoptimized in water (PCM) using three additional DFT functionals (M06-2X [32a], LC-TPSSTPSS [32b] and  $\omega$ B97XD [32c]).

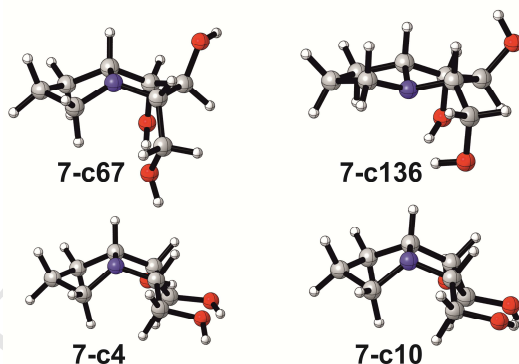


Figure 7. B3LYP/6-31G\* representative conformations of compound **7**

As shown in Table 1, despite the relative energies of the four species strongly depended on the level of theory, all functionals systematically predicted a higher stabilization of the **X<sub>ax</sub>** and **T** shapes over the **X/N** ones. Structure **7-c67** (**X<sub>ax</sub>** shaped) was the most stable according to SCF energy, whereas **7-c136** (**T** shaped) was generally the most stable according to Gibbs free energy calculations. On the other hand, the more “realistic” conformations **7-c4** and **7-c10** (featuring the required *pseudo*-diaxial H-2/H-3 protons) were much higher in energy (between 1.25-2.02 Kcal/mol).

**Table 2.** Relative SCF and Gibbs free energies (in parenthesis) of the conformers shown in Figure 7 after full geometry optimization in water (PCM) at the 6-311+G\*\* basis set.

Functional	Relative Energy (Kcal/mol)			
	<b>7-c67</b> ( <b>X<sub>ax</sub></b> )	<b>7-c136</b> ( <b>T</b> )	<b>7-c4</b> ( <b>X/N</b> )	<b>7-c10</b> ( <b>X/N</b> )
mPW1PW91 <sup>a</sup>	0.00	0.17	1.43	1.27
B3LYP	0.00 (1.39)	0.22 (0.00)	1.33 (2.12)	1.25 (1.86)
M06-2X	0.00 (0.00)	1.39 (0.51)	1.82 (1.57)	2.02 (1.73)
LC-TPSSTPSS	0.00 (0.02)	1.16 (0.00)	1.62 (1.19)	1.78 (1.33)
ωB97XD	0.00 (0.37)	0.64 (0.00)	1.82 (1.88)	1.66 (1.47)

a) Single point at PCM/mPW1PW91/6-31+G\*\*//B3LYP/6-31G\*

According to our results, the modest results experienced with compounds **6** and **7** might be the result of an artifact arising from the Boltzmann distributions computed at DFT level, overestimating the relative stability of unwished conformations (or alternatively, underestimating the relative stability of suitable ones).

To avoid such spurious conformations Navarro Vázquez and Gil have proposed a least-squares deconvolution of different ensembles of conformers followed by Akaike Information Criterion to select the optimal ensemble that explains the observed NMR data [16]. Despite this exciting approach performed nicely with molecules of low conformational freedom, the number of possible ensembles arising from highly flexible molecules would prevent its application in this case. On the other hand, we recently shown in a related case that the conflict exerted by H-bonding could be solved by total neglecting all questionable conformations [33]. We decided to follow this last approach by removing all those conformations of compounds **1-8** featuring a **T** shape and/or intramolecular bonding between the OH groups at C-1 and C-8. The NMR shifts were re-computed with the remaining ones following the standard approach to compute the conformational amplitudes by Boltzmann. In excellent agreement with our heuristic approach, the quality of the NMR prediction increased significantly (mainly for **6** and **7**, but for other isomers as well). As expected, such improvement was reflected in the corresponding DP4 and DP4+ probabilities. With DP4 the probabilities were more modest, but still much better than initially observed (Table 1). The only compound misassigned was still **5**, which was again identified in second place though with lower confidence. On the other hand, all the isomers under study were correctly assigned in high confidence (>95%) with DP4+, reinforcing our initial hypothesis.

**Table 3.** DP4 and DP4+ probabilities, and CMAE and CMaxErr values computed after correlating the experimental NMR data of compounds **1-3** and **5-8** with the calculated NMR shifts of **1-8** after removing all the **T** shapes and conformations showing intramolecular H-bonding between the OH groups at C-1 and C-8.

Comp.	Probability (rank) <sup>a</sup>	CMAE <sup>b</sup>		CMaxErr <sup>b</sup>	
		<sup>13</sup> C	<sup>1</sup> H	<sup>13</sup> C	<sup>1</sup> H
<b>DP4</b>					
<b>1</b>	>99.9 (1°)	1.1	0.12	2.2	0.35
<b>2</b>	75.9 (1°)	2.0	0.15	3.5	0.34
<b>3</b>	59.3 (1°)	1.4	0.15	3.8	0.43
<b>5</b>	0.3 (2°)	1.6	0.19	3.6	0.47
<b>6</b>	>99.9 (1°)	2.3	0.13	4.4	0.20
<b>7</b>	49.6 (1°)	1.8	0.18	3.7	0.35
<b>8</b>	>99.9 (1°)	1.9	0.14	3.6	0.33
<b>DP4+</b>					
<b>1</b>	>99.9 (1°)	1.5	0.12	3.9	0.41
<b>2</b>	>99.9 (1°)	1.5	0.10	3.5	0.31
<b>3</b>	97.7 (1°)	2.0	0.09	4.4	0.24
<b>5</b>	>99.9 (1°)	1.8	0.07	3.3	0.19
<b>6</b>	99.8 (1°)	2.4	0.13	4.3	0.25
<b>7</b>	98.7 (1°)	1.9	0.13	4.1	0.30
<b>8</b>	>99.9 (1°)	1.4	0.10	3.8	0.21

a) Indicates the ranked position of the correct isomer according to the probability values.

b) Computed by correlating the NMR data calculated for the corresponding isomer from which the experimental NMR were taken (ie. calcd. **1** vs exp. **1**)

To further explore the negative effect that few but highly stable structures in terms of NMR reproducibility, we recomputed the NMR shifts of compounds **1-8** by removing the most stable conformations regardless their shapes. Figure 8 shows the DP4+ values obtained after systematically discarding all conformations within 2 Kcal/mol (Ensemble A) and 4 Kcal/mol (Ensemble B) from the PCM/mPW1PW91/6-31+G\*\*//B3LYP/6-31G\* corresponding global minima. The number of remaining conformations were, in the average, 90% (Ensemble A), and 64% (Ensemble B).

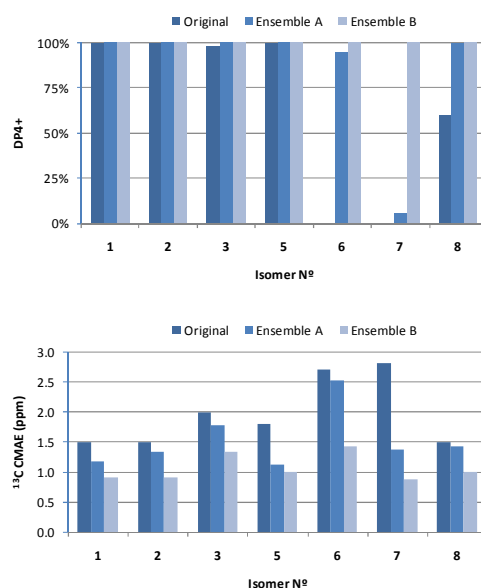


**Figure 8.** DP4+ (above) and <sup>13</sup>C-CMAE (below) values obtained for compounds **1-3** and **5-8** at the PCM/mPW1PW91/6-31+G\*\*//B3LYP/6-31G\* level of theory using three different ensembles of conformations: a) the full set of conformers, b) after removing all conformations within 2 Kcal/mol from the corresponding global minima (ensemble A), and c) after removing all conformations within 4 Kcal/mol from the corresponding global minima (ensemble B).

To our surprise, after this completely counterintuitive procedure the results significantly improved. In the case of ensemble A, the DP4+ values of **6** and **8** significantly jumped from <0.1% and 59.6% (original ensemble) to 94.5% and 99.5%, respectively. The results with compound **7** also increased, though in a more modest fashion (from <0.1% to 5.2%). Noteworthy, in ensemble B the corresponding DP4+ probabilities of these three isomers reached >99.9% values. On the other hand, the results obtained with the compounds correctly assigned by DP4+ in high confidence (**1**, **2**, **3** and **5**) with the original ensemble remained constant. In this regard, it is also important to point out that the  $^{13}\text{C}$  and  $^1\text{H}$  NMR shifts computed for **1-3** and **5-8** showed higher match with the experimental values of the corresponding isomer when using ensembles A and B (Figure 8).

Naturally, it would be extremely risky to suggest a new way of computing NMR shifts by systematic neglecting the most stable conformations found. However, the results herein presented showed a very interesting trend, suggesting that the wells on the potential surface are not as deep as estimated by standard DFT methods. In this regard, it should be emphasized the quest regarding the real conformational landscape of these compounds. In the light of the previous reports suggesting the **T** shapes as contributing conformations of substituted pyrrolizidines [29], it seemed clear that the removal of conflicting conformations was a shortcut to improve the NMR results. Current research are being undertaken to develop general DFT-based procedures to assign other members of the hyacinthacine family and will be published in due course.

### 3. Conclusion

We have thoroughly evaluated the performance of DP4 and DP4+ in the stereoassignment of hyacinthacines A1 and A2, and five other synthetic isomers. Our results showed that the quality of the predictions strongly depend on the ability of DFT methods to reproduce the conformational behavior of the system. Using the original ensemble of conformers (as determined by standard Boltzmann analysis), DP4+ correctly assigned five isomers, whereas the remaining two examples (compounds **6** and **7**) were found highly unlikely. Prompted by this unusual result, we explored the conformational landscape of these compounds and found that the drawback arose spurious intramolecularly H-bonded shapes arising from over-stabilized DFT energetics. In good agreement with this finding, we showed that the results significantly

improved upon removing such conflicting conformations, with all isomers being correctly classified by DP4+ in high probability (>99.9%). Similar trends were observed for DP4, though the results were more modest.

### Computational Details

All the DFT calculations were carried out using Gaussian 09 [34]. Systematic conformational searches were done with compounds **1-8** at the MMFF<sub>aq</sub> force field implemented in MacroModel [27]. All conformers found within a 10 Kcal/mol window from the corresponding global minima (1196 in total) were kept for NMR calculations at the B3LYP/6-31G\*\* level (for DP4 analysis). In addition, all these structures were submitted to full geometry optimizations at the PCM/B3LYP/6-31G\* level (using water as solvent), including frequency calculations to identify the nature of the stationary points found. After removing duplicates, all the remaining structures (1037 in total) were used as inputs for NMR calculations at the PCM/mPW1PW91/6-31+G\*\* level of theory, the recommended for DP4+ analysis [19], using water as solvent. The isotropic shielding values ( $\sigma$ ) were computed using the gauge including atomic orbitals (GIAO) method [35], the recommended one to tackle the gauge origin problem for organic molecules [12]. The calculations in solution were carried out using the polarizable continuum model, PCM [36], with water as the solvent. The unscaled chemical shifts ( $\delta_u$ ) were calculated with TMS as reference standard according to  $\delta_u = \sigma_x - \sigma_{\text{TMS}}$ , where  $\sigma_x$  is the Boltzmann averaged isotropic shielding value of nucleus  $x$  and  $\sigma_{\text{TMS}}$  is the isotropic shielding value of TMS computed at the same level of theory. The Boltzmann averaging was done at room temperature (298 K) using the SCF relative energies extracted from the NMR calculation stage (B3LYP/6-31G\*\*//MMFF in case of DP4 and PCM/mPW1PW91/6-31+G\*\*//B3LYP/6-31G\* in case of DP4+). The scaled chemical shifts ( $\delta_s$ ) were obtained as  $\delta_s = (\delta_u - b)/m$ , where  $m$  and  $b$  are the slope and intercept, respectively, resulting from a linear regression calculation on a plot of  $\delta_u$  vs  $\delta_{\text{exp}}$ . The DP4 calculations were carried out using a home-made Excel file built with the statistical parameters originally reported [14], and the DP4+ calculations were carried out using the Excel spreadsheet available for free at sarotti-NMR.weebly.com, or as part of the Supporting Information of the original paper [19].

## Acknowledgements

This research was supported by UNR (BIO 316 and BIO 500), ANPCyT (PICT-2016-0116), and PhosAgro/UNESCO/IUPAC (Green Chemistry for Life Program, project 121).

## Supplementary Data

Supplementary data to this article is available free of charge at DOI: xxxx, and includes experimental and calculated data of compounds **1-8**, DP4 and DP4+ probabilities and MMFF<sub>aq</sub> and B3LYP/6-31G\* Cartesian coordinates (with energies) of all compounds.

## References

- [1] B.L. Stocker, E.M. Dangerfield, A.L. Win-Mason, G.W. Haslett, M.S. Timmer, Recent Developments in the Synthesis of Pyrrolidine-Containing Iminosugars, *Eur. J. Org. Chem.* 2010 (2010) 1615-1637.
- [2] S.G. Pyne, M. Tang, The structure, biological activities and synthesis of 3-hydroxylpyrrolizidine alkaloids and related compounds, *Curr. Org. Chem.* 9 (2005) 1393-1418.
- [3] J. Robertson, K. Stevens, Pyrrolizidine alkaloids: occurrence, biology, and chemical synthesis. *Nat. Prod. Rep.* 34(1) (2017) 62-89.
- [4] A.A. Watson, G.W. Fleet, N. Asano, R.J. Molyneux, R.J. Nash, Polyhydroxylated alkaloids-natural occurrence and therapeutic applications, *Phytochem.* 56 (2001) 265-295
- [5] T. Ritthiwigrom, C. W. G Au, S. G Pyne, Structure, biological activities and synthesis of hyacinthacine alkaloids and their stereoisomers, *Curr. Org. Synth.* 9 (2012) 583-612.
- [6] [a] T.L. Suyama, W.H. Gerwick, K.L. McPhail, Survey of marine natural product structure revisions: A synergy of spectroscopy and chemical synthesis, *Bioorg. Med. Chem.* 19 (2011) 6675-6701.[b] K. Nicolaou, S.A. Snyder, Chasing molecules that were never there: misassigned natural products and the role of chemical synthesis in modern structure elucidation, *Angew. Chem., Int. Ed.* 44 (2005) 1012-1044.
- [7] A. Kato, N. Kato, I. Adachi, J. Hollinshead, G.W. Fleet, C. Kuriyama, K. Ikeda, N. Asano, R.J. Nash, Isolation of glycosidase-inhibiting hyacinthacines and related alkaloids from *Scillasocialis*, *J. Nat. Prod.* 70 (2007) 993-997.
- [8] A. Kato, I. Adachi, M. Miyauchi, K. Ikeda, T. Komae, H. Kizu, Y. Kameda, A.A. Watson, R.J. Nash, M.R. Wormald, Polyhydroxylatedpyrrolidine and pyrrolizidine alkaloids from *Hyacinthoides non-scripta* and *Scillacampanulata*, *Carbohydr. Res.* 316 (1999) 95-103.

- [9] [a] K. Savasapun, C.W.G. Au, S.G. Pyne, Total Synthesis of Hyacinthacines B3, B4, and B5 and Purported Hyacinthacine B7, 7-epi-Hyacinthacine B7, and 7a-epi-Hyacinthacine B3 from a Common Precursor, *J. Org. Chem.* 79 (2014) 4569-4581. [b] W. Christopher, Synthesis of hyacinthacine B3 and purported hyacinthacine B7, *Chem. Commun.* 46 (2010) 713-715. [c] T. Sengoku, Y. Satoh, M. Takahashi, H. Yoda, Total synthesis of the proposed structures of hyacinthacines C2, C3, and their C5-epimers, *Tetrahedron Lett.*, 50 (2009) 4937-4940. [d] W. Zhang, K. Sato, A. Kato, Y.-M. Jia, X.-G. Hu, F.X. Wilson, R. van Well, G. Horne, G.W.J. Fleet, R.J. Nash, C.-Y. Yu, Synthesis of Fully Substituted Polyhydroxylated Pyrrolizidines via Cope–House Cyclization, *Org. Lett.*, 13 (2011) 4414-4417. [e] J. A. Tamayo, F. Franco, F. Sánchez-Cantalejo, Synthesis of the Proposed Structure of Pentahydroxylated Pyrrolizidine Hyacinthacine C5 and Its C6,C7 Epimer, *Eur. J. Org. Chem.* 2011 (2011) 7182-7188. [f] T. Pecchioli, F. Cardona, H.-U. Reissig, R. Zimmer, A. Goti, Alkoxyallene-Based Stereodivergent Syntheses of (–)-Hyacinthacine B4 and of Putative Hyacinthacine C5 Epimers: Proposal of Hyacinthacine C5 Structure, *J. Org. Chem.* 82 (2017) 5835-5844.
- [10] A.W. Carroll, K. Savasapun, A.C. Willis, M. Hoshino, A. Kato, S.G. Pyne, Total Synthesis of Natural Hyacinthacine C5 and Six Related Hyacinthacine C5 Epimers, *J. Org. Chem.* 83 (2018) 5558-5576.
- [11] [a] J. Calveras, J. Casas, T. Parella, J. Joglar, P. Clapés, Chemoenzymatic Synthesis and Inhibitory Activities of Hyacinthacines A1 and A2 Stereoisomers, *Advanced Synthesis & Catalysis*, 349 (2007) 1661-1666. [b] X. Garrabou, L. Gómez, J. Joglar, S. Gil, T. Parella, J. Bujons, P. Clapés, Structure-Guided Minimalist Redesign of the L-Fucose-1-Phosphate Aldolase Active Site: Expedient Synthesis of Novel Polyhydroxylated Pyrrolizidines and their Inhibitory Properties Against Glycosidases and Intestinal Disaccharidases, *Chem. Eur. J.* 16 (2010) 10691-10706.
- [12] For leading reviews, see: [a] N. Grimblat, A.M. Sarotti, Computational Chemistry to the Rescue: Modern Toolboxes for the Assignment of Complex Molecules by GIAO NMR Calculations, *Chem. Eur. J.* 22 (2016) 12246-12261. [b] D.J. Tantillo, Questions in natural products synthesis research that can (and cannot) be answered using computational chemistry, *Chemical Society Reviews*, 47 (2018) 7845-7850. [c] M.W. Lodewyk, M.R. Siebert, D.J. Tantillo, Computational prediction of  $^1\text{H}$  and  $^{13}\text{C}$  chemical shifts: A useful tool for natural product, mechanistic, and synthetic organic chemistry, *Chem. Rev.* 112 (2011) 1839-1862 [d] A. Bagno, G. Saielli, Addressing the stereochemistry of complex organic molecules by density functional theory-NMR, *Wiley Interdisciplinary Rev. Comp. Mol. Sci.* 5 (2015) 228-240. [e] D.J. Tantillo, Walking in the woods with quantum chemistry—applications of quantum chemical calculations in natural products research, *Nat. Prod. Rep.* 30 (2013) 1079-1086. [f] G. Bifulco, P. Dambrosio, L. Gomez-Paloma, R. Riccio, Determination of relative configuration in organic compounds by NMR spectroscopy and computational methods, *Chem. Rev.* 107 (2007) 3744-3779 [g] A. Navarro-Vázquez, State of the art and perspectives in the application of quantum chemical prediction of  $^1\text{H}$  and  $^{13}\text{C}$  chemical

shifts and scalar couplings for structural elucidation of organic compounds, *Magn. Reson. Chem.* 55 (2017) 29-32.

[13] S.G. Smith, J.M. Goodman, Assigning the stereochemistry of pairs of diastereoisomers using GIAO NMR shift calculation, *J. Org. Chem.*, 74 (2009) 4597-4607.

[14] S.G. Smith, J.M. Goodman, Assigning stereochemistry to single diastereoisomers by GIAO NMR calculation: the DP4 probability, *J. Am. Chem. Soc.*, 132 (2010) 12946-12959.

[15] [a] A.M. Sarotti, Successful combination of computationally inexpensive GIAO  $^{13}\text{C}$  NMR calculations and artificial neural network pattern recognition: a new strategy for simple and rapid detection of structural misassignments, *Org. Biomol. Chem.* 11 (2013) 4847-4859. [b] M.M. Zanardi, A.M. Sarotti, GIAO C-H COSY Simulations Merged with Artificial Neural Networks Pattern Recognition Analysis. Pushing the Structural Validation a Step Forward, *J. Org. Chem.*, 80 (2015) 9371-9378.

[16] [a] E. Troche-Pesqueira, C. Anklin, R.R. Gil, A. Navarro-Vázquez, Computer-Assisted 3D Structure Elucidation of Natural Products using Residual Dipolar Couplings, *Angew. Chem. Int. Ed.*, 56 (2017) 3660-3664. [b] A. Navarro-Vázquez, R.R. Gil, K. Blinov, Computer-assisted 3D structure elucidation (CASE-3D) of natural products combining isotropic and anisotropic NMR parameters, *J. Nat. Prod.*, 81 (2018) 203-210.

[17] A.G. Kutateladze, D.S. Reddy, High-throughput in silico structure validation and revision of halogenated natural products is enabled by parametric corrections to DFT-computed  $^{13}\text{C}$  NMR chemical shifts and spin-spin coupling constants, *J. Org. Chem.* 82 (2017) 3368-3381

[18] D. Xin, P.-J. Jones, N.C. Gonnella, D i CE: Diastereomeric in Silico Chiral Elucidation, Expanded DP4 Probability Theory Method for Diastereomer and Structural Assignment, *J. Org. Chem.* 83 (2018) 5035-5043.

[19] N. Grimblat, M.M. Zanardi, A.M. Sarotti, Beyond DP4: an Improved Probability for the Stereochemical Assignment of Isomeric Compounds using Quantum Chemical Calculations of NMR Shifts, *J. Org. Chem.*, 80 (2015) 12526-12534.

[20] [a] M.M. Zanardi, A.G. Suarez, A.M. Sarotti, Determination of the Relative Configuration of Terminal and Spiroepoxides by Computational Methods. Advantages of the Inclusion of Unscaled Data, *J. Org. Chem.* 82 (2017) 1873-1879. [b] M.M. Zanardi, F.A. Biglione, M.A. Sortino, A.M. Sarotti, General Quantum-Based NMR Method for the Assignment of Absolute Configuration by Single or Double Derivatization: Scope and Limitations, *J. Org. Chem.* 83 (2018) 11839-11849.

[21] [a] N. Grimblat, T.S. Kaufman, A.M. Sarotti, Computational Chemistry Driven Solution to Rubriflordilactone B, *Org. Lett.*, 18 (2016) 6420-6423. [b] A.M. Sarotti,

Structural revision of two unusual rhamnofolanediterpenes, curcusones I and J, by means of DFT calculations of NMR shifts and coupling constants, *Org. Biomol. Chem.* 16 (2018) 944-950.

[22] G. Oruc, T. Varnali, S. Bekiroglu, Hydroxy protons as structural probes to reveal hydrogen bonding properties of polyols in aqueous solution by NMR spectroscopy, *J. Mol. Struct.* 1160 (2018) 319-327.

[23] I.G. Shenderovich, Simplified calculation approaches designed to reproduce the geometry of hydrogen bonds in molecular complexes in aprotic solvents, *J. Chem. Phys.* 148 (2018) 124313.

[24] A. Bagno, F. Rastrelli, G. Saielli, Prediction of the  $^1\text{H}$  and  $^{13}\text{C}$  NMR spectra of  $\alpha$ -D-glucose in water by DFT methods and MD simulations, *J. Org. Chem.* 72 (2007) 7373-7381.

[25] F.V. Toukach, V.P. Ananikov, Recent advances in computational predictions of NMR parameters for the structure elucidation of carbohydrates: methods and limitations, *Chem. Soc. Rev.* 42 (2013) 8376-8415.

[26] For the NMR data of 1 (A1) and 2 (A2), see: [a] N. Asano, H. Kuroi, K. Ikeda, H. Kizu, Y. Kameda, A. Kato, I. Adachi, A.A. Watson, R.J. Nash, G.W. Fleet, New polyhydroxylated pyrrolizidine alkaloids from *Muscariarmeniaceum*: structural determination and biological activity, *Tetrahedron: Asymmetry*, 11 (2000) 1-8. For the NMR data of 3, 6 and 7, see Ref. [11a], with compounds 3 and 6 initially reported as 5 and 4, respectively, further revised in Ref. [11b]. For the NMR data of 5, see Ref. [11b]. For the NMR data of 8, see: [b] I. Izquierdo, M.T. Plaza, J.A. Tamayo, F. Franco, F. Sánchez-Cantalejo, Total synthesis of natural (+)-hyacinthacine A6 and non-natural (+)-7*a*-*epi*-hyacinthacine A1 and (+)-5, 7*a*-*diepi*-hyacinthacine A6, *Tetrahedron* 66 (2010) 3788-3794.

[27] MacroModel Schrodinger release 2018-3; Schrodinger LLC: New York, 2018.

[28] [a] C. Culvenor, M. Heffernan, W. Woods, Nuclear magnetic resonance spectra of pyrrolizidine alkaloids. I. The spectra of retronecine and heliotridine, *Aust. J. Chem.*, 18 (1965) 1605-1624. [b] C. Culvenor, W. Woods, Nuclear magnetic resonance spectra of pyrrolizidine alkaloids. II. The pyrrolizidine nucleus in ester and non-ester alkaloids and their derivatives, *Aust. J. Chem.*, 18 (1965) 1625-1637.

[29] [a] I. Skvortsov, Cis-trans-conversion of the bicycle in pyrrolizidines: The effect of the preferred conformations on the properties of the bases and the thermodynamics of conformational transformation of the ring fusion type, *Chem. Het. Comp.* 42 (2006) 1247-1266. [b] I. Skvortsov, Investigations on 1-Azabicyclic Compounds. 25. Stereochemistry, Hydrogen Bonds, and Gas-Liquid Chromatography of Pyrrolizidine Alcohols, *Chem. Het. Comp.* 39 (2003) 493-503.

- [30] A.M. Belostotskii, E. Markevich, Conformational dynamics in nitrogen-fused azabicycles, *J. Org. Chem.* 68 (2003) 3055-3063.
- [31] G.I. Csonka, A.D. French, G.P. Johnson, C.A. Stortz, Evaluation of Density Functionals and Basis Sets for Carbohydrates, *J. Chem. TheoryComput.* 5 (2009) 679-692.
- [32] [a] Y. Zhao, D.G. Truhlar, The M06 suite of density functionals for main group thermochemistry, thermochemical kinetics, noncovalent interactions, excited states, and transition elements: two new functionals and systematic testing of four M06-class functionals and 12 otherfunctionals, *Theor. Chem. Acc.* 120 (2008) 215-241.[b]J. Tao, J.P. Perdew, V.N. Staroverov, G.E. Scuseria, Climbing the density functional ladder: Nonempirical meta-generalized gradient approximation designed for molecules and solids, *Phys. Rev. Lett.* 91 (2003) 146401.[c]J.-D. Chai, M. Head-Gordon, Long-range corrected hybrid density functionals with damped atom-atom dispersion corrections, *Phys. Chem. Chem. Phys.* 10 (2008) 6615-6620.
- [33] P. Huang, C. Li, A.M. Sarotti, J. Turkson, S. Cao, Sphaerialactonam, a  $\gamma$ -lactam-isochromanone from the Hawaiian endophytic fungus *Paraphaeosphaeria* sp. FT462, *Tetrahedron Lett.* 58 (2017) 1330-1333.
- [34] M. J. Frisch, G. W. Trucks, H. B. Schlegel, G. E. Scuseria, M. A. Robb, J. R. Cheeseman, G. Scalmani, V. Barone, B. Mennucci, G. A. Petersson, H. Nakatsuji, M. Caricato, X. Li, H. P. Hratchian, A. F. Izmaylov, J. Bloino, G. Zheng, J. L. Sonnenberg, M. Hada, M. Ehara, K. Toyota, R. Fukuda, J. Hasegawa, M. Ishida, T. Nakajima, Y. Honda, O. Kitao, H. Nakai, T. Vreven, J. A. Montgomery Jr., J. E. Peralta, F. Ogliaro, M. J. Bearpark, J. Heyd, E. N. Brothers, K. N. Kudin, V. N. Staroverov, R. Kobayashi, J. Normand, K. Raghavachari, A. P. Rendell, J. C. Burant, S. S. Iyengar, J. Tomasi, M. Cossi, N. Rega, N. J. Millam, M. Klene, J. E. Knox, J. B. Cross, V. Bakken, C. Adamo, J. Jaramillo, R. Gomperts, R. E. Stratmann, O. Yazyev, A. J. Austin, R. Cammi, C. Pomelli, J. W. Ochterski, R. L. Martin, K. Morokuma, V. G. Zakrzewski, G. A. Voth, P. Salvador, J. J. Dannenberg, S. Dapprich, A. D. Daniels, Ö. Farkas, J. B. Foresman, J. V. Ortiz, J. Cioslowski, D. J. Fox *Gaussian 09* (Gaussian Inc, Wallingford, CT, 2009).
- [35] [a] R. Ditchfield, Molecular orbital theory of magnetic shielding and magnetic susceptibility, *J. Chem. Phys.* 56 (1972) 5688-5691.[b]R. Ditchfield, Self-consistent perturbation theory of diamagnetism: I. A gauge-invariant LCAO method for NMR chemical shifts, *Mol. Phys.* 27 (1974) 789-807.[c] C.M. Rohlfing, L.C. Allen, R. Ditchfield, Proton and carbon-13 chemical shifts: comparison between theory and experiment, *Chem. Phys.*, 87 (1984) 9-15.[d] K. Wolinski, J.F. Hinton, P. Pulay, Efficient implementation of the gauge-independent atomic orbital method for NMR chemical shift calculations, *J. Am. Chem. Soc.* 112 (1990) 8251-8260.
- [36] J. Tomasi, B. Mennucci, R. Cammi, Quantum mechanical continuum solvation models, *Chem. Rev.* 105 (2005) 2999-3093

- Hyacinthacines are important members of the pyrrolizidine family
- Several hyacinthacines have ambiguous, revised or unverified structures
- We explored DP4 and DP4+ in the stereoassignment of seven known hyacinthacines
- The quality of the predictions strongly depended on the conformational preferences
- Removing spurious conformations with intramolecular H-bonding improved the results